IOPscience iopscience.iop.org

Home Search Collections Journals About Contact us My IOPscience

The Effects of Low-Pressure Rapid Thermal Post-Annealing on the Properties of (Ba, Sr)TiO_3 Thin Films Deposited by Liquid Source Misted Chemical Deposition

This content has been downloaded from IOPscience. Please scroll down to see the full text.

2001 Jpn. J. Appl. Phys. 40 L1333

(http://iopscience.iop.org/1347-4065/40/12A/L1333)

View the table of contents for this issue, or go to the journal homepage for more

Download details:

IP Address: 140.113.38.11
This content was downloaded on 28/04/2014 at 05:29

Please note that terms and conditions apply.

Jpn. J. Appl. Phys. Vol. 40 (2001) pp. L 1333–L 1335
Part 2, No. 12A, 1 December 2001
©2001 The Japan Society of Applied Physics

The Effects of Low-Pressure Rapid Thermal Post-Annealing on the Properties of $(Ba,Sr)TiO_3$ Thin Films Deposited by Liquid Source Misted Chemical Deposition

Ming-Jui YANG, Chao-Hsin CHIEN, Ching-Chich LEU, Ren-Jian ZHANG[1], Shich-Chuan WU, Tiao-Yuan HUANG and Tseung-Yuen TSENG[1]

National Nano Device Laboratories, Hsinchu 30050, Taiwan, R.O.C.
[1]*Institute of Electronics, National Chiao Tung University, Hsinchu 30050, Taiwan, R.O.C.*

(Received August 27, 2001; accepted for publication October 11, 2001)

The technique of low-pressure post-annealing process with additional second-step annealing for preparation of the $Ba_{0.7}Sr_{0.3}TiO_3$ thin films deposited by liquid source misted chemical deposition (LSMCD) has been proposed. With employing this annealing procedure, the leakage current density can be significantly eliminated by approximately one order of magnitude at 2 V. In particular, process temperature can be reduced from 650°C to 600°C without suffering deteriorated crystallinity issue, which is identified by both C–V measurement and X-ray diffraction spectrum. The extracted dielectric constant is 310 with extreamly low loss tangent of 0.005. The spectrum of atomic force microscopy (AFM) shows that this low-pressure process results in smoother surface topography. Moreover, thermal desorption spectrums assure that less residual organics and contaminations were left after low pressure post-annealing. This may be one of the reasons for lowering crystallization temperature and the improved electrical properties.

KEYWORDS: $(Ba,Sr)TiO_3$, LSMCD, low pressure rapid thermal post-annealing, process temperature, leakage current density, residue organics

The projected capacitor area in the dynamic random access memory (DRAM) cell is rapidly shrinking as the integration density increases. The required capacitance for assuring stable circuit operation and sufficient soft-error immunity, which is at 25 fF/cell, could be achieved either by reducing the thickness of the dielectric films or by increasing the effective surface area of the capacitor electrodes. However, neither approach seems to be practical to next-generation of ULSI DRAMs fabrication because of the unacceptable leakage current increase and the extreamely complicated integration process, respectively. Therefore, the incorporation of new dielectric material with high dielectric constant becomes the most likely alternative approach for the coming giga-bit dynamic random access memories. Recently, $(Ba,Sr)TiO_3$ (BST) with excellent dielectric properties, such as large dielectric constant, low dielectric dissipation factor, and low leakage current level, has attracted extensive attention for the application in next generation ULSI DRAMs.[1,2] Although many techniques have succeeded in depositing high-quality BST thin films, for example, rf-magnetron sputtering, pulsed laser ablation, and metal-organic chemical vapor deposition (MOCVD),[3–5] liquid source misted chemical deposition (LSMCD), in particular, has been proved to be an simple and inexpensive alternative technique with the capability of precise composition control and excellent step coverage.[6,7] In this paper, we study the effects of low-pressure rapid thermal post-annealing on the properties of BST thin films deposited by LSMCD. It has been found that low-pressure rapid thermal post-annealing can lower down the BST film crystallization temperature by 50°C and, moreover, reduce leakage current by near one order of magnitude at 2 V.

The $Ba_{0.7}Sr_{0.3}TiO_3$ films prepared by LSMCD method were deposited on $Pt/SiO_2/Si$ substrates. The as-deposited samples were subjected to drying at 150°C to remove the residual solvent and then pyrolysis at 400°C for 10 min. The desired BST film thickness of about 100 nm was achieved through multiple repetitions of the process sequence. Subsequently, some samples accepted rapid thermal annealing in atmospheric oxygen ambient at 650°C for 1 min and others, for comparison, were performed with low-pressure oxygen rapid thermal annealing at 50 Torr and 600°C for 10 min. For electrical measurements, Pt top electrodes were deposited onto BST films through a shadow mask with a diameter of 0.2 mm. After the top electrode formation, additional second-step annealing at 600°C for 30 min in air was selectively applied to the samples. The electrical properties and reliability characteristics of the metal oxide were measured by using a Hewlett-Packard (HP) 4156 semiconductor parameter analyzer. X-ray diffraction (XRD) was also used to identify the composition and the phase of these new metal oxide films. Surface morphologies of BST thin films were characterized by atomic force microscope (AFM). The residual gases and contamination left inside the bulk of thin films were detected by thermal desorption spectrums (TDS).

The electrical properties of deposited BST thin films are shown in Fig. 1. Figure 1(a) exhibits the leakage current densities and Fig. 1(b) shows both the dielectric constants and dissipation factors of BST thin films as a function of applied top gate bias for various annealing conditions. In Fig. 1(a), the sample annealed at 760 Torr and 650°C for 1 min shows a slightly higher leakage current than that with low pressure post-annealing at lower temperature in the low field regime. However, there is no obvious difference above the knee between these two samples. The leakage current densities are around 3.1E-7 A/cm^2 at 2 V. On the other hand, the leakage current density of the sample subjected to low-pressure annealing is found tremendously suppressed with additional second-step annealing at 600°C in air for both relaxation and Schottky emission currents. The current density is about 4.45×10^{-8} A/cm^2 at 2 V, which is almost one order of magnitude improvement compared to the previous samples. The impacts of low-pressure process on the BST thin film are further identified by the film capacitance behavior, as shown in Fig. 1(b). The trend is very different from that of leakage current. The capacitance decreases dramatically for the sample treated with only one-step low-pressure post-annealing. As we added

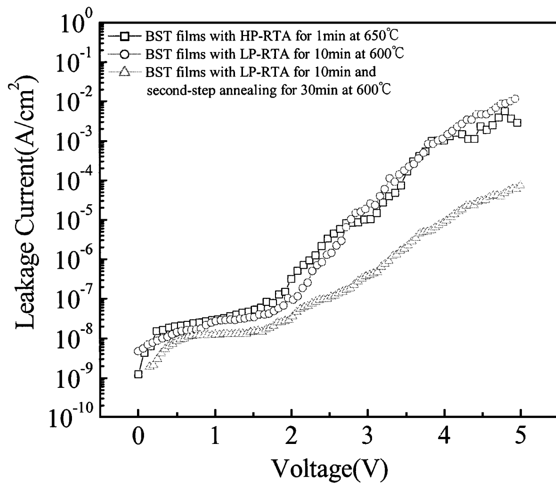

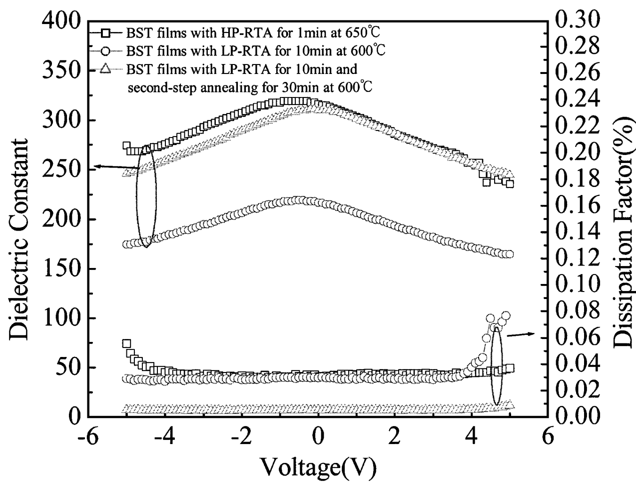

Fig. 1. (a) Leakage current densities, (b) dielectric constants and dissipation factors as a function of the applied bias voltage for the samples various annealing conditions.

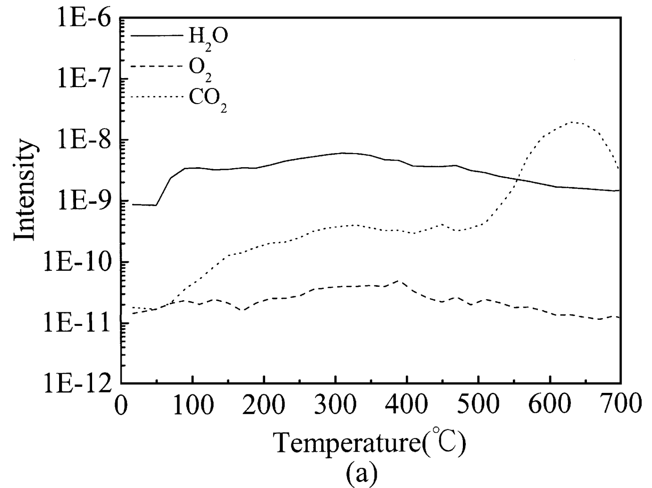

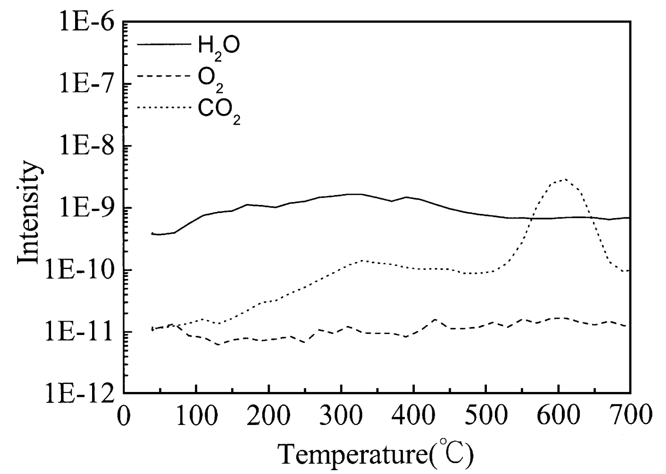

Fig. 2. TDS spectra of BST thin films after (a) 760 Torr for 1 min at 650°C (b) 50 Torr for 10 min at 600°C.

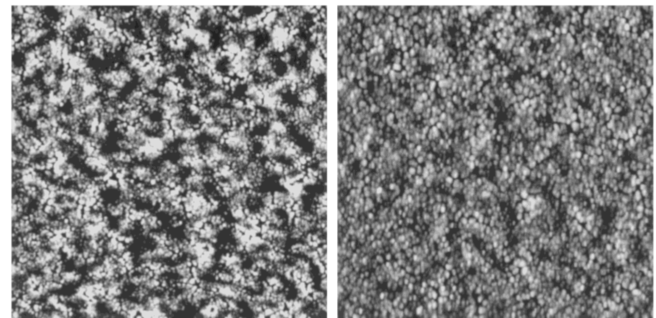

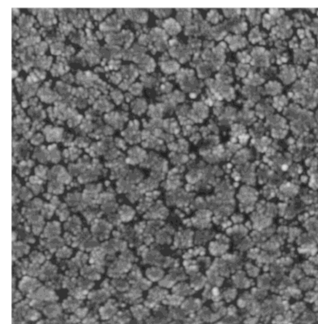

Fig. 3. AFM images of BST thin films after (a) 50 Torr for 10 min at 600°C (b) 50 Torr for 10 min and the second-step annealing for 30 min at 600°C (c) 760 Torr for 1 min at 650°C.

second-step annealing, the film capacitance is almost recovered and dissipation factor becomes even ramarkably smaller. The capacitance recovery is speculated to the microstructure transformation of BST films and will be discussed later. The dissipation factor is believed to closely related to the leakage current density, thus the films subjected to 2-step low-pressure annealing showed lower dielectric loss.

In order to obtain the picture of the detailed mechanism about the film improvement by low-pressure annealing procedure, the impurities contained in the bulk, surface morphology and microstructure of BST thin films were analyzed with thermal desorption spectrum, atomic force microscope and X-ray diffraction spectrum, respectively. Figure 2 shows the level of residual organics and contamination, including CO_2, H_2O and O_2, left in the BST films after high- and low-pressure annealing conditions by TDS. It is clearly seen that low-pressure annealing can more efficiently remove residual organics and contamination. Figure 3 shows the surface morphologies of the BST thin films with various heat treatment sequences. Both thin films subjected to low-pressure annealing, shown in Figs. 3(a) and 3(b), exhibit much smoother surface morphologies than that of thin film with 1 atm post-annealing. The values of surface roughness are seperately

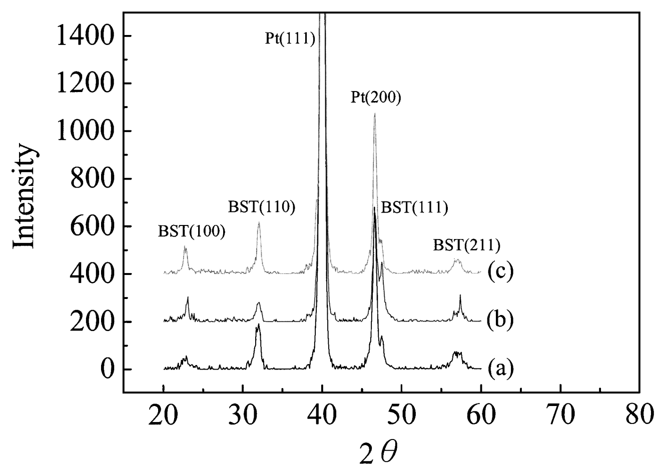

Fig. 4. XRD patterns of BST thin films after (a) 760 Torr for 1 min. at 650°C (b) 50 Torr for 10 min. at 600°C (c) 50 Torr for 10 min and the second-step annealing for 30 min at 600°C.

1.839 nm, 2.122 nm, and 2.738 nm. However, without second step annealing, abundant porosities have been observed in the film. The addition of another annealing in air at the same temperature has been found to successfully eliminate the number of porosity and make the film structure much denser. According to the previous reports the leakage current consists of two components, i.e., relaxation current and Schottky emission current. It is believed that relaxation current is strongly correlated to the concentration of impurities and oxygen vacancies in the bulk, while Schottky emission current is mainly dictated by the film/electrode interface quality.[8–11] From our leakage current results, we speculate that the variations due to different heat treatments are ascribed to the plenty of oxygen vacancies produced in thin films during the lower-pressure annealing step. Although low-pressure annealing process is beneficial for removing the residual organics and contamination contained in thin films,[12–14] it would also induce more oxygen atoms evaporated at the same time and then create oxygen vacancies distributed in thin films during crystallization. While smoother surface has been obtained, those generated oxygen vacancies can deteriorate the film crystalline microstructure and make them more porous. Consequently, no improvement has been achieved in the film J–V characteristic. Therefore, our intention of employing additional second-step annealing is trying to provide the required oxygen and energy to recovery vacancies.[14] The results do show that additional annealing can make thin film denser without causing significant increase of surface roughness, which lead to reduction of both relaxation and Schottky emission currents.

Figure 4 shows XRD patterns of those corresponding BST thin films. From these spectra, we try to find out the origin of the capacitance behaviors induced by low-pressure annealing. As we can see, the thin film with 760 Torr, 650°C post-annealing exhibits a strong (110) texture. In contrast, low-pressure annealing favors the preferential growth of (111) texture and would be converted into (110) oriented texture by the additional post-annealing in air at 600°C. Consistent with previous reports, the development of stronger (110)-oriented BST thin film does show better crystallinity and higher dielectric constant.[15–17] Thus, we believe that these preferred orientations of the films with distinct heat treatments contribute to the variations of the film capacitance behavior.

In summary, a new low-pressure processing with the second-step annealing technique for preparation of the $Ba_{0.7}Sr_{0.3}TiO_3$ thin films deposited by LSMCD has been proposed. Not only lower crystallization temperature but also more excellent electrical properties can be obtained by this newly developed method. The improvement is believed due to the less remain of residual organics and contamination in the BST thin film, the smoother and denser film structure and reduction of oxygen vacancies. Therefore, this method is very useful for achieving highly integrated memory applications.

1) Y. Ohno, T. Horikawa, H. Shinkawata, K. Kashihara, T. Kuroiwa, T. Okudaira, Y. Hashizume, K. Fukumoto, T. Eimori, T. Shibano, K. Arimoto, H. Itoh, T. Nishimura and H. Miyoshi: *Proc. Symp. VLSI Technology, 1994*, p. 149.
2) K. Takemura, T. Sakuma and Y. Miyasaka: Appl. Phys. Lett. **64** (1994) 2967.
3) C. M. Chu and P. Lin: Appl. Phys. Lett. **70** (1997) 249.
4) S. Yoon and A. Safari: J. Appl Phys. **76** (1994) 2999.
5) C. S. Chern, S. Liang, Z. Q. Shi, S. Yoon, A. Safari, P. Lu, B. H. Kear, B. H. Goodreau, T. J. Marks and S. Y. Hou: Appl. Phys. Lett. **64** (1994) 3181.
6) M. Huffman: Integr. Ferroelectr. **10** (1995) 39.
7) H. J. Chung, J. H. Kim, W. S. Moon, S. B. Park, C. S. Hwang, M. Y. Lee and S. I. Woo: Integr. Ferroelectr. **12** (1996) 185.
8) T. Horikawa, T. Makita, T. Kuroiwa and N. Mikami: Jpn. J. Appl. Phys. **34** (1995) 5478.
9) S. O. Park, C. S. Hwang, H. J. Cho, C. S. Kang, H. K. Kang, S. I. Lee and M. Y. Lee: Jpn. J. Appl. Phys. **35** (1996) 1548.
10) Y. Fukuda, H. Haneda, I. Sakaguchi, K. Numata, K. Aoki and A. Nishimura: Jpn. J. Appl. Phys. **36** (1997) L1514.
11) Y. Fukuda, K. Numata, K. Aoki, A. Nishimura, G. Fujihashi, S. Okamura, S. Ando and T. Tsukamoto: Jpn. J. Appl. Phys. **37** (1998) L453.
12) Y. Ito, M. Ushikubo, S. Yokoyama, H. Matsunaga, T. Atsuki, T. Yonezawa and K. Ogi: Jpn. J. Appl. Phys. **35** (1996) 4925.
13) N. Ogata, M. Nagata, K. Ishihara, H. Urashima, A. Okutoh, S. Yamazaki, S. Mitarai and J. Kudo: Jpn. J. Appl. Phys. **37** (1998) 3481.
14) Y. Fujimori, T. Nakamura and H. Takasu: Jpn. J. Appl. Phys. **38** (1999) 5346.
15) T. Horikawa, N. Mikami, T. Makita, J. Tanimura, M. Kataoka, K. Sato and M. Nunoshita: Jpn. J. Appl. Phys. **32** (1993).
16) S. Y. Cha, H. C. Lee, W. J. Lee and H. G. Kim: Jpn. J. Appl. Phys. **34** (1995) 5220.
17) J.-G. Cheng, X.-J. Meng, B. Li, J. Tang, S.-L. Guo and J.-H. Chu: Appl. Phys. Lett. **75** (1999) 2132.